86

STRUCTURAL AND FUNCTIONAL BRAIN IMAGING OF ALZHEIMER DISEASE

GARY W. SMALL

Of the many laboratory measures and techniques available for understanding and quantifying biological aspects of *Alzheimer disease* (AD), imaging the structure and function of the brain is a particularly attractive approach in that it can provide highly relevant and diverse information using a variety of techniques. The application and interpretation of such information have considerable practical clinical relevance, but as these technologies and our understanding of the disease pathogenesis continue their rapid evolution, so do the potential utilities of these imaging methods in addressing timely neuropsychopharmacologic research issues.

Brain imaging techniques are often categorized as either structural or functional, based on the primary form of information provided. This classification method breaks down, however, when considering newer applications of these techniques. For example, magnetic resonance imaging (MRI) equipment is used to provide functional brain responses with functional MRI (fMRI). Moreover, both positron emission tomography (PET) and single photon emission computed tomography (SPECT) have the potential to provide visualizations of the pathognomonic structural lesions of AD, the amyloid neuritic plaques (NPs), and neurofibrillary tangles (NFTs).

The *in vivo* visualization of relevant structures and functions through brain imaging has several clinical and research applications for AD and other dementias. Recognition of dementia is particularly difficult in its early stages, when family members and physicians often incorrectly attribute the patient's symptoms to normal aging (1,2). Systematic studies indicate that the frequency of unrecognized memory impairment, beyond that associated with normal aging, or a dementia diagnosis can range from 50% to 90% of cases (3,4). A related application is the differential diagnosis of various dementia causes. The gradual onset and progressive cognitive decline of AD may be difficult to distinguish clinically from other chronic dementias, including dementia with Lewy bodies, vascular dementia, frontotemporal dementia, and late-life depression. Brain imaging techniques may sort out these various causes. The marginal diagnostic value (i.e., added specificity and sensitivity) that a brain imaging procedure provides also has applications to neuropharmacologic clinical trials. When brain imaging improves diagnostic homogeneity, drug efficacy and safety studies are likely to be more informative.

Another application of brain imaging is in the preclinical detection of AD. Neuropathologic, neuropsychological, and brain imaging data point to a form of gradual age-related cognitive decline that precedes AD (5). Use of imaging studies, particularly when coupled with data on genetic risk of AD, is an emerging strategy to identify candidates for pharmacologic interventions that delay cognitive decline progression and disease onset. A related application is the use of brain imaging data to predict and follow treatment response in patients with the full dementia syndrome of AD. Finally, imaging studies also may provide information that clarifies underlying disease mechanisms, which, in turn, may foster improved drug development. In this chapter, I review both available and developing brain imaging techniques and emphasize neuroimaging techniques and measures for presymptomatic AD detection and monitoring pharmacologic interventions.

STRUCTURAL NEUROIMAGING TECHNIQUES

Computed Tomography

Computed tomography (CT) measures the attenuation of an x-ray beam through body tissues. A tissue's appearance will vary according to its attenuation. Bone has the highest attenuation and appears white, whereas gas has the lowest

Gary A. Small: Department of Psychiatry and Biobehavioral Sciences, Neuropsychiatric Institute, Alzheimer's Disease Centers, Center on Aging, University of California; Veterans Affairs Greater Los Angeles Healthcare System, Los Angeles, California.

and appears black. A ring of x-ray generators and detectors obtains images of multiple brain slices as the patient is advanced through the scanner (6). CT can differentiate bone, soft tissue, fluid, and gas with spatial resolution of less than 1 mm. Intravenous contrast medium enhances such pathologic features as bleeding, neoplasm, infection, and inflammation. Limitations of CT include its inability to differentiate gray and white matter and to visualize the posterior fossa clearly (6). Quantitative CT measures have demonstrated greater brain atrophy and ventricular dilatation in patients with AD compared with controls (7). The rate of clinical decline in AD is also related to the rate of ventricular volume change (8).

Magnetic Resonance Imaging

MRI measures the radiofrequency energy that hydrogen atoms of water molecules emit. In a static magnetic field, lower-energy nuclei align with the field, whereas higher-energy nuclei align against the field. When irradiated at a specific frequency, some lower-energy nuclei absorb energy and align against the field. The MRI scanner detects energy emitted when the radiation is discontinued and the nuclei return to their lower-energy state (9). Such energy level changes provide measures of brain structure representations. The rate that nuclei return to their low-energy state determines the type of image produced: T1-weighted images differentiate gray and white matter, and T2 images delineate white matter hyperintensities (9). Because MRI does not involve ionizing radiation, patients can have multiple scans. Spatial resolution is 1 to 2 mm, usually less than that of CT. Much of the work using MRI has focused on regional volumetric changes in patients with AD compared with controls, with an emphasis on atrophy of the hippocampus and nearby medial temporal structures (10).

FUNCTIONAL NEUROIMAGING TECHNIQUES

Quantitative Electroencephalography

The development of computer-analyzed EEGs and the ability to examine regional differences in EEG activity have potential applications to the study of dementia (11). Quantitative EEG coherence measures the synchronization of neuronal activity at two different cortical sites. If different brain areas are simultaneously activated during a task, coherence between these areas will increase. In AD, reductions in resting state coherence occur between intrahemispheric parietal and prefrontal cortical areas, whereas in vascular dementia, reduction in coherence occurs between occipital and parietal areas (12). Changes in coherence in both the resting state and during task performance may become techniques for the differential diagnosis of dementia. Advantages of quantitative EEG are availability, low cost, and lack of radiation exposure. Disadvantages include the possibility of artifact and the fact that the measures are relatively distant from the brain. Moreover, the precise physiologic meaning of the measure is unclear. Resting state coherence in specific areas can be reduced in AD and in vascular dementia. In AD, the greatest reductions in coherence occur between intrahemispheric parietal and prefrontal cortical areas, whereas in vascular dementia, this reduction occurs between occipital and parietal areas (13).

Single Photon Emission Computed Tomography

SPECT involves administration of an inhaled or injected tracer or unstable isotope. Tracer decay leads to single photon emission, the scanner determines the site of the photon source, and a computer generates a three-dimensional image reflecting cerebral blood flow or receptor distribution (14). In comparison with PET, SPECT has lower spatial resolution, particularly for imaging deep structures. Moreover, determining the source of single photon emitters is less precise compared with determining the two photons traveling in opposite directions in PET scanning. Unlike PET, SPECT cannot demonstrate glucose metabolism.

Positron Emission Tomography

PET tracers are positron-emitting nuclides. When a positron encounters an electron, the positron is destroyed and releases photons traveling in opposite directions. A scanner records the simultaneous arrival of two different photons at different detectors (180 degrees apart) and determines the line along which the photons travel. PET images are then constructed from information received by the scanner (15). PET, like SPECT, delineates cerebral blood flow and receptor characteristics. Injection of high-affinity receptor ligands labeled with nuclides can measure receptor density and affinity. Studies of AD often use fluorodeoxyglucose (FDG) to measure cerebral glucose metabolism, which reflects synaptic activity. PET studies have demonstrated characteristic alterations in cerebral blood flow and metabolism in patients with AD that begin in the parietal cortex and spread to the temporal and prefrontal cortices. The degree of hypometabolism correlates with the severity of cognitive impairment (16). PET images can differentiate patients with AD from patients with other dementias and from cognitively intact people (17).

Although investigators have focused considerable attention on the cholinergic system in AD, numerous other neurotransmitter systems are affected, and PET has been used to study them. For example, striatal uptake of the dopamine reuptake ligand [11C]β-CFT is decreased in AD, a finding indicating involvement of the brain dopaminergic system (18). In addition to serotonergic deficits (19), cholinergic

nicotinic and muscarinic receptors have been studied using PET radioligands (20).

Both PET and SPECT are noninvasive procedures that demonstrate neuronal activity or receptor characteristics. Advantages of PET include its better spatial resolution and the type of biological information it provides. Because of their radiochemical characteristics, positron emitters (PET tracers) can produce more ligands than photon emitters (SPECT tracers) for receptor studies. Lower scanner costs and greater availability of PET tracers have led to wider availability.

Magnetic Resonance Spectroscopy

Nuclei produce magnetic fields that modify the fields of neighboring atoms of the same molecule. Such ''shielding'' produces a small variation in the resonant frequency known as a chemical shift. The magnetic resonance spectrum display according to frequency demonstrates an element's different chemical forms as characteristic peaks. These spectroscopy displays provide information on biologically important elements, thus reflecting tissue metabolite concentrations (21). Magnetic resonance spectroscopy (MRS) is noninvasive, lacks ionizing radiation exposure, and can provide quantitative regional measures of biochemical and physiologic processes. Schuff and associates used proton MRS (1H MRS) and tissue-segmented and volumetric MRI to determine whether hippocampal *N*-acetylaspartate (NAA, a neuronal marker) and volume used together provided greater discrimination between patients with AD and normal elderly persons than either measure alone (22). These investigators found that NAA reductions and volume losses made independent contributions to the discrimination of patients with AD from controls. Concentrations of myoinositol- and choline-containing compounds are higher in the occipital and parietal regions of adults with Down syndrome compared with controls (23).

Functional Magnetic Resonance Imaging

Developments in MRI techniques have allowed investigators to use the device to measure brain activity. The altered MRI signal intensity reflects local changes in blood volume or blood flow. The signal intensity of deoxygenated hemoglobin (highly paramagnetic) differs from that of oxygenated hemoglobin. During brain activity, increased blood flow brings more oxygenated blood into the capillary bed. The brain does not metabolize this excess oxygen, and this causes a greater concentration of oxygenated blood to cross over to the venous side leading to a decrease in the magnetic field gradient at the capillaries. The resultant greater magnetic field homogeneity yields a higher MRI signal intensity. Thus, brain regions receiving greater blood flow during brain activity produce a stronger MRI signal than do other regions. By comparing perfusion in activated and nonactivated states, areas of relative brain activity can be identified (24). Thus, fMRI provides measures of signal intensity that are associated with relative cerebral blood flow during memory or other cognitive tasks (25–30), and it has the advantages of high resolution in space and time and lack of radiation exposure. The MRI signal intensity associated with a particular task in comparison with the control condition reflects blood flow and consequently neural activity, but only indirectly (31,32). fMRI studies of patients with AD reveal lowered brain activity in parietal and hippocampal regions and relatively higher activity in primary cortices unaffected by the disease (33).

Diffusion Tensor Imaging

A critical aspect of the interpretation of normal and abnormal brain function is neuronal connectivity. One method that provides visualizations of projections of axonal fibers is diffusion tensor MRI (34). The technique offers quantitative information on the directionality (anisotropy) of water diffusion and thus information on local fiber orientation and integrity of white matter tracks. Diffusion tensor imaging (DTI) quantifies and visualizes diffusional anisotropy within each voxel, and computer algorithms relate DTI data to three-dimensional projections of axonal fibers. The degree of neuronal connectivity loss observed in AD is clearly a useful measure to monitor as the disease progresses, and combining DTI with other imaging modalities (e.g., PET, fMRI) may be a useful approach, which has been described in other neuropsychiatric disorders (35). A DTI study of diffusion anisotropy of pyramidal tract in ten older and ten younger adults subjects found that older persons had lower values in the cerebral peduncle, with no differences in the pons and medulla (36). A study of hippocampal water diffusion changes and temporal white matter using DTI in patients with AD and controls suggests that decreased fiber density occurs early in the temporal white matter, probably related to secondary degeneration from gray matter disease of the medial temporal lobe (37). Moreover, studies using DTI indicate mild myelin loss in patients with AD, even though white matter appears normal on MRI, and areas of periventricular hypertrophy show a definite loss of myelin and axons, including incomplete infarction (38).

IMAGING ANALYSIS TOPICS RELEVANT TO DEMENTIA RESEARCH

Numerous variables influence the methodologic error introduced into imaging studies of dementia, including the stability and resolution of imaging systems, the reliability of image analysis, the effect size, undefined neuropathology, the stage of illness, and various confounding factors. The particular method of image analysis provides different levels of image detail and sources of error.

Imaging Registration

In early studies of SPECT and PET imaging, regions of interest (ROIs) were drawn directly on the PET images, matched to a standard atlas. This approach has high interrater reliability (39), but better anatomic definition is possible with computer software that provides image overlay programs merging structural and functional imaging data within the same subject for ROI analyses (40). Such algorithms also allow alignment of multiple PET images obtained from a single subject (41). Registration of PET images that have uniform three-dimensional resolution permits direct regional metabolic comparisons, whereas MRI and PET registration allows precise anatomic localization of those metabolic data in terms of the individual's structural anatomy.

Statistical Parametric Mapping

In statistical parametric mapping (SPM) analysis (42,43), images are coregistered and reoriented into a standardized coordinate system, spatially smoothed, and normalized to mean global activity. The set of pooled data are then assessed on a voxel-by-voxel basis, to identify the profile of voxels that significantly change between conditions (e.g., baseline versus follow-up scan). The probability of finding by chance any region containing its voxel of maximal significance is assessed after adjusting for multiple comparisons. It is not surprising that results vary according to analytic method. The ROI approach depends on *a priori* assumptions on size and shape of regions defined by structural criteria. If functionally relevant areas deviate from *a priori* assumptions, an area not functionally involved will dilute the statistical effect. By contrast, SPM analysis relies on pooled brain images spatially normalized into a common space; the extent that the original size and shapes of brains differ will inevitably introduce some error. Minoshima and colleagues applied an automated image analysis method, wherein metabolic reductions were standardized using three-dimensional stereotactic surface projections from FDG PET scans of patients with AD compared with controls (44). This approach has been useful in studies of asymptomatic subjects at risk of developing AD (45).

Atrophy Correction

Decreased functional imaging signal intensity in patients with AD may result from local atrophy causing partial volume effects. Approaches to correcting for cerebral atrophy and partial volume effects include a binary method, wherein cerebrospinal fluid (CSF) and brain tissue are segmented and the composite tissue images are convolved to the in-plane resolution of the PET image. The binary method ignores averaging between gray matter and white matter, and pathologic and imaging data suggest gray matter losses in AD greater than white matter losses (46). In trinary correction methods, CSF, gray matter, and white matter segmentation are included (47) (Fig. 86.1). Computer simulation studies (47) have shown close to 100% recovery of radiotracer concentration in neocortical gray matter and hippocampus, and they indicate that errors in gray matter segmentation and errors in registration of PET and MRI images result in less than 15% inaccuracy in the corrected image. Other work indicates that the neocortical deficits observed in AD reflect true metabolic reductions and are not just the result of atrophy (48).

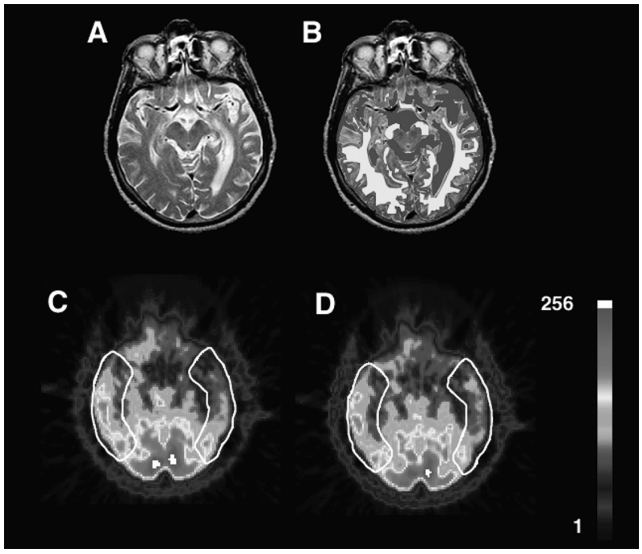

FIGURE 86.1. Partial volume correction using the trinary method. Example of the method using MRI and FDG PET images of a patient with primary progressive aphasia and left (seen on the **right** in figure image planes viewed from below the subject's head) temporal atrophy. Trinary segmentation (gray matter, white matter, CSF) was performed on the MRI image at the level of the temporal lobe. The MRI image was then registered and resliced to align with the PET image. The corrected left temporal glucose metabolic rate was higher than the uncorrected left temporal glucose metabolic rate, an expected result in light of the left temporal lobe atrophy. The corrected and uncorrected glucose metabolic raters for the right temporal lobe were nearly the same, consistent with the minimal atrophic changes in the right hemisphere. **A:** MRI scan without tissue segmentation. **B:** MRI scan with tissue segmentation (*yellow,* white matter; *gray,* gray matter; *blue,* CSF). **C:** Uncorrected PET image (*white lines* indicate temporal region of interest) showing left-to-right temporal lobe asymmetry of glucose metabolic rate. **D:** Corrected PET image showing less striking asymmetry. (Courtesy of Dr. Henry Huang, Department of Molecular and Medical Pharmacology, UCLA School of Medicine, Los Angeles.) See color version of figure.

USE OF NEUROIMAGING FOR PRESYMPTOMATIC AD DETECTION AND PHARMACOLOGIC TREATMENT MONITORING

During the past decade, investigators have been focusing their efforts on early detection of AD at clinical stages before

the time when a physician confirms a clinical diagnosis of probable AD (49). The aim is to begin preventive pharmacologic treatments before extensive neuronal damage develops. Brain imaging has become an important tool for the development of surrogate markers that will effectively identify people with only mild cognitive losses who are likely to progress in their cognitive loss and who will eventually develop the full dementia syndrome of AD. As novel, disease-modifying agents emerge, these surrogate brain imaging markers will be critical in determining drug efficacy and will facilitate drug development in both animal models and human studies.

Several diagnostic entities have been described in efforts to characterize age-related cognitive decline better. The mildest form of age-related memory decline is known as age-associated memory impairment (AAMI) (50), characterized by self-perception of memory loss and a standardized memory test score greater than or equal to 1 standard deviation (SD) below the aged norms. In people 65 years of age or older, its estimated prevalence is 40%, afflicting approximately 16 million people in the United States (51). Only about 1% of such patients develop dementia each year. A more severe form of memory loss is mild cognitive impairment (MCI), often defined by significant memory deficits without functional impairments. People with MCI show memory impairment that is greater than or equal to 1.5 SD below aged norms on such memory tasks as delayed paragraph recall (52). Approximately 10% of people 65 years old or older suffer from MCI, and nearly 15% develop AD each year (52,53). Brain imaging studies of presymptomatic AD focus on both these forms of age-related memory decline.

Evidence of Presymptomatic Disease

Neuropathologic, neuroimaging, and clinical research supports the idea that the dementing process leading to AD begins years before a clinical diagnosis of probable AD can be confirmed (49). Postmortem studies of nondemented older people indicate that tangle density in healthy aging correlates with age (54), but that some persons demonstrate widely distributed neuritic and diffuse plaques throughout neocortex and limbic structures. Other studies have found that NFT density increases in some persons (55), presumably those who will eventually develop AD, very early in adult life, perhaps even by the fourth decade. The diffuse amyloid deposits in middle-aged nondemented persons are consistent with an early or ''preclinical'' stage of AD and suggest that the pathologic process progresses gradually, taking 20 to 30 years to proceed to the clinical manifestation of dementia (56). Other supportive evidence includes findings that linguistic ability in early life predicts cognitive decline in late life (57). High diffuse plaque density in nondemented older persons has been observed in the entorhinal cortex and inferior temporal gyrus, in association with acetylcholinesterase fiber density (58). Evidence from animal models also supports compromised hippocampal cholinergic transmission during aging (59). Studies of glucose metabolic rates using PET (45,60,61) indicate lower regional brain metabolism in middle-aged and older persons with a genetic risk (apolipoprotein E-4 [APOE-4]), lending further support to a prolonged presymptomatic AD stage.

Structural Imaging

Computed Tomography and Magnetic Resonance Imaging

Studies of early detection logically follow from initial work demonstrating the differential diagnostic utility of a brain imaging marker. For structural imaging, particularly MRI, data have emerged on the use of regional atrophy patterns for the positive diagnosis of AD and other neurodegenerative disorders. Studies without neuropathologic confirmation report the utility of medial temporal lobe atrophy, particularly hippocampal atrophy, on CT or MRI for the clinical diagnosis of AD (62). Some, but not all, quantitative MRI studies indicate that white matter hyperintensities correlate with neuropsychological functioning in both healthy elderly persons and demented patients (63,64). Other studies indicate loss of cerebral gray matter (46), hippocampal and parahippocampal atrophy (65), and lower left amygdala and entorhinal cortex volumes (66) in patients with AD. In differentiating AD from older normal controls, the sensitivity of various medial temporal atrophy measures ranges from 77% to 92%, with specificities ranging from 49% to 95% (67–69). In older patients with MCI, hippocampal atrophy predicts subsequent conversion to AD (70). Of various analytic methods, computerized volumetric techniques are most accurate, but they are currently labor intensive and are not widely available.

A modified negative-angle axial view designed to cut parallel to the anterior-posterior plane of the hippocampus has been used to assess hippocampal volume using CT or MRI (62). Such hippocampal atrophy is a sensitive and specific predictor of future AD in patients with MCI. Baseline hippocampal ratings accurately predicted decliners with an overall accuracy of 91%. Neuropathologic studies found that the sites of maximal neuronal loss for both AD and MCI are in the CA1, subiculum, and entorhinal cortex (62). Hippocampal atrophy was also found to predict future cognitive decline in older persons without cognitive impairment who were followed-up for nearly 4 years. Visual assessments of medial temporal lobe atrophy on coronal MRI sections show significant correlations between estimated and stereologically measured volumes (71). Because the latter is much more labor intensive, visual readings may be an alternative approach with greater efficiency.

The hippocampus and the temporal horn of the lateral ventricles also may serve as antemortem AD markers in

mildly impaired patients (mean Mini-Mental State Examination [MMSE] score of 24) (72). Although hippocampal atrophy may enable one to distinguish AD from normal aging, such atrophy may be nonspecific, occurring in other dementing disorders (73). MRI hippocampal atrophy measures are not as sensitive as PET glucose metabolism measures, which begin decreasing before the onset of memory decline (74). The presence of MRI white matter hyperintensities does not improve diagnostic accuracy because they occur both in AD and in healthy normal elderly persons (75,76).

The entorhinal cortex, a region involved in recent memory performance, is one of the earliest areas to accumulate NFTs (55). Histologic boundaries of the entorhinal cortex from patients with autopsy-confirmed AD and controls have been used to validate a method for measurement of entorhinal cortex size relying on gyral and sulcal landmarks visible on MRI (77). Such measures may be additional early AD detection markers.

Several studies have addressed the interaction between regional atrophy and *APOE* genotype. Increasing dose of *APOE-4* allele was associated with smaller hippocampal, entorhinal cortical, and anterior temporal lobe volumes in already demented patients (78). A study of nondemented older persons found an association between *APOE-4* dose and a larger left than right hippocampus (79). Combining medial temporal measures with other functional neuroimaging (80) or *APOE* genotyping may improve the ability of any of these measures alone to predict cognitive decline (81).

In Vivo Imaging of Amyloid Plaques and Neurofibrillary Tangles

The evidence of NP and NFT accumulation years before clinical AD diagnosis suggests that *in vivo* methods that directly image these pathognomic lesions would be useful presymptomatic detection technologies. Current methods for measuring brain amyloid, such as histochemical stains, require tissue fixation on postmortem or biopsy material. Available *in vivo* methods for measuring NPs or NFTs are indirect (e.g., CSF measures) (82). Studies that may lead to direct *in vivo* human Aβ imaging include various radiolabeled probes using small organic and organometallic molecules capable of detecting differences in amyloid fibril structure or amyloid protein sequences (83). Investigators also have used chrysamine-G, a carboxylic acid analogue of congo red, an amyloid-staining histologic dye (84), serum amyloid P component, a normal plasma glycoprotein that binds to amyloid deposit fibrils (85), or monoclonal antibodies (86). Methodologic difficulties that hinder progress with these techniques include poor blood–brain barrier crossing and limited specificity and sensitivity. In addition, most approaches do not measure both NPs and NFTs.

In a breakthrough, Barrio and colleagues (87) used a hydrophobic radiofluorinated derivative of 1,1-dicyano-2-[6-(dimethylamino)naphthalen-2-yl]propene (FDDNP) (88) with PET to measure the cerebral localization and load of NFTs and SPs in patients with AD (n = 7) and controls (n = 3). The FDDNP was injected intravenously and was found to cross the blood–brain barrier readily in proportion to blood flow, as expected from highly hydrophobic compounds with high membrane permeability. Greater accumulation and slower clearance of FDDNP were observed in brain regions with high concentrations of NPs and NFTs, particularly the hippocampus, amygdala, and entorhinal cortex. The FDDNP residence time in these regions showed significant correlations with immediate and delayed memory performance measures (89), and areas of low glucose metabolism correlated with high FDDNP activity retention. The probe showed visualization of NFTs, NPs, and diffuse amyloid in AD brain specimens using *in vitro* fluorescence microscopy, which matched results using conventional stains (e.g., thioflavin S) in the same tissue specimens. Thus, FDDNP-PET imaging is a promising noninvasive approach to longitudinal evaluation of NP and NFT deposition in preclinical AD.

Magnetic Resonance Spectroscopy

Initial studies of MRS as a preclinical AD detection technique found significantly lower NAA concentrations in persons with AD and AAMI compared with controls (90). Mean inositol concentration was significantly higher in AD than in controls, whereas persons with AAMI had intermediate values. Another study focused on patients with Down syndrome because they invariably develop AD by the time they reach their thirties or forties. Concentrations of myoinositol- and choline-containing compounds found using 1H MRS were significantly higher in the occipital and parietal regions in 19 nondemented adults with Down syndrome and in 17 age- and sex-matched healthy controls (23). Moreover, older patients with Down syndrome (42 to 62 years) had higher myoinositol levels than younger subjects (28 to 39 years), a finding suggesting that this approach may be eventually useful as a preclinical AD marker.

Functional Imaging

Positron Emission Tomography

Using FDG PET, our group reported that parietal hypometabolism predicted future AD in people with questionable dementia (91), and even people with very mild age-related memory complaints have baseline PET patterns predicting cognitive decline after 3 years (92). These initial studies using PET for early AD detection emphasized family history of AD as a risk factor for future cognitive decline. A change in focus came with the discovery of the *APOE* genetic risk for AD. The first report combining PET imaging and *APOE*

genetic risk in people with a family history of AD included 12 nondemented relatives with *APOE*-4 and 19 relatives without *APOE*-4 and compared them with seven patients with probable AD (61). "At-risk" subjects had mild memory complaints, normal cognitive performance, and at least two relatives with AD. Persons with *APOE*-4 did not differ from those without *APOE*-4 in mean age at examination (56.4 versus 55.5 years) or in neuropsychologic performance. Parietal metabolism was significantly lower and left-right parietal asymmetry was higher in at-risk subjects with *APOE*-4 compared with those without *APOE*-4. Patients with dementia had significantly lower parietal metabolism than did at-risk persons with *APOE*-4.

The following year, Reiman and associates replicated these results and extended them to other brain regions (45). These investigators found hypometabolism in temporal, prefrontal, and posterior cingulate regions in a study of 11 nondemented *APOE*-4 homozygotes (4/4 genotype) and in 22 *APOE*-3 homozygotes (3/3 genotype) of similar ages to those in our own initial study (midfifties). They also applied an automated image analysis method, wherein metabolic reductions were standardized using three-dimensional stereotactic surface projections from FDG PET scans of patients with AD compared with controls (44). The results from these two studies (45,61) provided independent confirmation of an association between genetic risk and regional cerebral glucose hypometabolism.

Our group confirmed these two initial reports in a study that included none of the subjects participating in our previous report on *APOE* and PET (61), in a study of 65 persons in the 50- to 84-year age range (mean $\pm$ = 67.3 ± 9.4 years), with or without a family history of AD (93). Of the 65 study subjects, 54 were nondemented (27 were *APOE*-4 carriers and 27 were subjects without *APOE*-4), and 11 were demented and were diagnosed with probable AD (49). The nondemented study subjects were aware of a gradual onset of mild memory complaints (e.g., misplacing familiar objects, difficulty in remembering names). The nondemented subjects, however, had memory performance scores within the norms for cognitively intact persons of the same age and educational level. The *APOE*-4 carriers had a small but consistent nonsignificant reduction in cognitive performance. As predicted, baseline comparisons among the three subject groups indicated the lowest metabolic rates for the AD group, intermediate rates for the nondemented *APOE*-4 carriers, and highest rates for the nondemented group without *APOE*-4 in several cortical regions, including inferior parietal, lateral temporal, and posterior cingulate (Fig. 86.2).

Another FDG PET study focused on older patients with Down syndrome who were at risk of AD (94). The investigators hypothesized that an audiovisual stimulation paradigm would serve as a stress test and would reveal abnormalities in parietal and temporal cerebral glucose metabolism before dementia developed. At mental rest, younger and older patients with Down syndrome did not differ in glucose metabolic patterns. During audiovisual stimulation, however, the older patients showed significantly lower parietal and temporal metabolism. Families with familial AD linked to chromosome 14 or amyloid precursor protein (*APP*) mutations have been studied with FDG PET as well (95). In such families with early-onset AD, approximately half of relatives who live to the age at risk will develop AD. Although pedigree members with AD show typical parietal and temporal hypometabolism, asymptomatic relatives at risk of AD show a similar but less severe hypometabolic pattern.

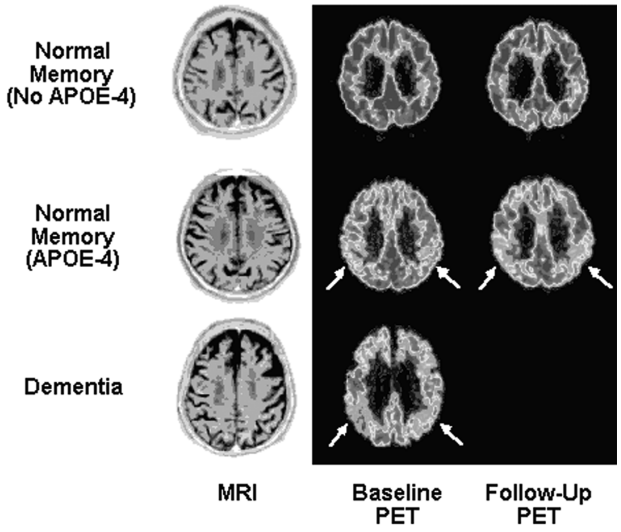

FIGURE 86.2. Examples of PET images (comparable parietal lobe levels) coregistered to each subject's baseline MRI scan for an 81-year-old nondemented woman (*APOE*-3/3 genotype; **upper images**), a 76-year-old nondemented woman (*APOE*-3/4 genotype; **middle images**), and a 79-year-old woman with AD (*APOE*-3/4 genotype; **lower images**). The last column shows 2-year follow-up scans for the nondemented women. Compared with the nondemented patient without *APOE*-4, the nondemented *APOE*-4 carrier had 18% **(right)** and 12% **(left)** lower inferior parietal cortical metabolism, whereas the demented woman's parietal cortical metabolism was 20% **(right)** and 22% **(left)** lower, as well as more widespread metabolic dysfunction resulting from disease progression. Two-year follow-up scans showed minimal parietal cortical decline for the woman without *APOE*-4, but bilateral parietal cortical decline for the nondemented woman with *APOE*-4, who also met clinical criteria for mild AD at follow-up. MRI scans were within normal limits. (From Small GW, Ercoli LM, Silverman DHS, et al. Cerebral metabolic and cognitive decline in persons at genetic risk for Alzheimer's disease. *Proc Natl Acad Sci USA* 2000;97:6037–6042, with permission.) See color version of figure.

Single Photon Emission Computed Tomography

Johnson and associates (96) used SPECT with technetium-hexamethylpropyleneamineoxime (HMPAO) to study longitudinal cerebral perfusion of patients with questionable AD (clinical dementia rating = 0.5) (97) and controls. Regional decreases in perfusion in patients whose diagnosis

converted to AD were most prominent in the hippocampal-amygdaloid complex, the anterior and posterior cingulate, and the anterior thalamus. Including *APOE* status did not influence results. A direct comparison of FDG PET and HMPAO-SPECT in their ability to differentiate AD from vascular dementia indicated higher diagnostic accuracy for PET regardless of dementia severity (98). Using ROC curves, PET diagnostic accuracy was better than SPECT for an MMSE score greater than 20 (87.2% versus 62.9%) and for an MMSE score less than or equal to 20 (100% versus 81.2%). Other studies confirmed a lower sensitivity for even high-resolution SPECT compared with PET (99). Moreover, the parietal hypoperfusion observed using SPECT in patients with AD has been observed in such other conditions as normal aging, vascular dementia, posthypoxic dementia, and sleep apnea (100).

Functional Magnetic Resonance Imaging

Two studies combined *APOE* genotyping and fMRI in persons at risk of AD. Bookheimer and associates (101) performed fMRI studies while 30 cognitively intact middle-aged and older persons (mean age, 63 years) memorized and retrieved unrelated word pairs. The 16 *APOE*-4 carriers did not differ significantly from the 14 persons without *APOE*-4 in age, prior educational achievement, or rates of AD family history. Brain activation patterns were determined during both learning and retrieval task periods and were analyzed using between-group and within-subject approaches. Memory performance was reassessed on 12 subjects after 2 years of follow-up. The *APOE*-4 carriers had significantly greater magnitude and spatial extent of MRI signal intensity during memory performance in regions affected by AD, including bilateral hippocampal and left parietal and prefrontal (Fig. 86.3). This pattern of activation was greater in the left hemisphere, consistent with the verbal nature of the task, and during the retrieval rather than the learning condition. Longitudinal data indicated that greater baseline brain activation correlated with verbal memory decline assessed 2 years later. The greater signal in persons with the *APOE*-4 genetic risk suggests that the brain may recruit additional neurons to compensate for subtle deficits. Moreover, the longitudinal data are encouraging that fMRI may be a useful approach to prediction of future cognitive decline and early AD detection.

By contrast, other types of memory tasks may produce different patterns of brain activation. In another study of persons at risk for AD, visual naming and letter fluency tasks were used to activate brain areas involved in object and face recognition during fMRI scanning (102). Subjects in the high-risk group had at least one first-degree relative with AD and one *APOE*-4 allele. The low-risk group was matched for age, education, and cognitive performance. The high-risk group showed reduced activation in the middle and posterior inferotemporal regions bilaterally. Such decreased activation patterns could result from subclinical neuropathology in the inferotemporal region or in the inputs to that region.

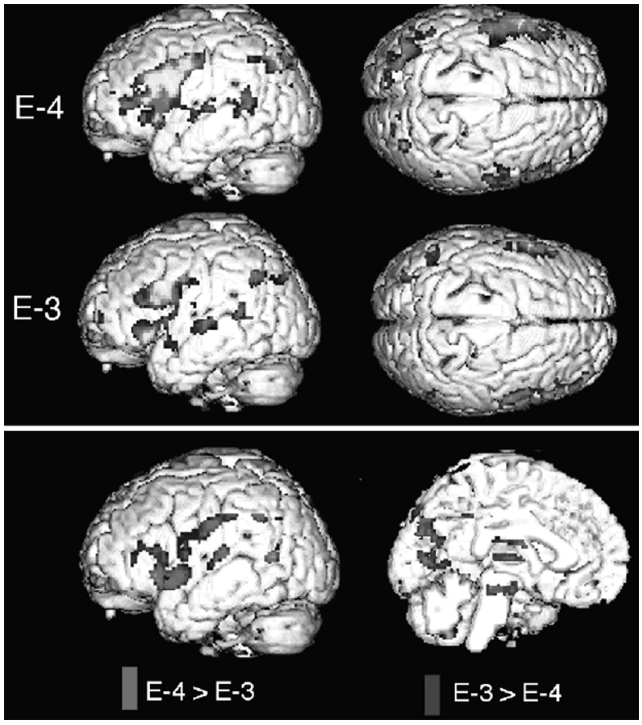

FIGURE 86.3. Statistical parametric maps of recall versus control blocks for *APOE*-4 carriers and noncarriers. Maps were standardized into a common coordinate system. Both groups showed significant MRI signal intensity increases in frontal, temporal, and parietal regions, and the *APOE*-4 group had greater extent and intensity of activation. The *APOE*-4 group showed additional activations in the left parahippocampal region, left dorsal prefrontal cortex, and other regions in the inferior and superior parietal lobes, and anterior cingulate. (From Bookheimer SY, Strojwas MH, Cohen MS, et al. Brain activation in older people at genetic risk for Alzheimer's disease. *N Engl J Med* 2000;343:450–456, with permission.) See color version of figure.

Longitudinal Studies of Glucose Metabolism of Persons At Risk of Dementia

Both the University of California, Los Angeles (UCLA) and the University of Arizona groups have reported on longitudinal FDG PET follow-up data on nondemented persons at risk of AD. At UCLA, a total of 20 nondemented subjects (ten *APOE*-4 carriers and ten without *APOE*-4) received repeat PET and neuropsychologic testing 2 years after baseline assessment (mean $\pm$ SD for follow-up was 27.9 ± 1.7 months) (93). The ten *APOE*-4 carriers available for longitudinal study were similar to the ten noncarriers in mean $\pm$ SD age (67.9 ± 8.9 versus 69.6 ± 8.1 years) and educational achievement (14.4 ± 1.8 versus 16.4 ± 2.8 years). Memory performance scores did not differ signifi-

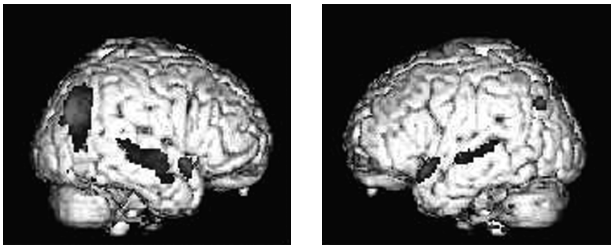

FIGURE 86.4. Regions showing the greatest metabolic decline after 2 years of longitudinal follow-up in nondemented patients with *APOE*-4 (SPM analysis) included the right lateral temporal and inferior parietal cortex (brain on the **left side** of the figure). Voxels undergoing metabolic decline ($p < .001$, before correction) are displayed in color, with peak significance ($z = 4.35$) occurring in Brodmann's area 21 of the right middle temporal gyrus. (From Small GW, Ercoli LM, Silverman DHS, et al. Cerebral metabolic and cognitive decline in persons at genetic risk for Alzheimer's disease. *Proc Natl Acad Sci USA* 2000; 343:450–456, with permission.) See color version of figure.

cantly according to genetic risk either at baseline or follow-up, and the *APOE*-4 carriers and noncarriers did not differ significantly in cognitive change after 2 years.

The ROI analysis of PET scans performed after 2 years showed significant glucose metabolic decline (4%) in the left posterior cingulate region in *APOE*-4 carriers. The SPM analysis showed significant metabolic decline in the inferior parietal and lateral temporal cortices with the greatest magnitude (5%) of metabolic decline in the temporal cortex (Fig. 86.4). After correction for multiple comparisons, this decline remained significant for the *APOE*-4 group, wherein a decrease in metabolism was documented for every subject. Based on these data from only ten subjects, the estimated power of PET under the most conservative circumstances is 0.9 to detect a one-unit decline from baseline to follow-up using a one-tailed test. Such findings suggest that combining PET and AD genetic risk measures will allow investigators to use relatively small sample sizes when testing antidementia treatments in preclinical AD stages. The University of Arizona group also found that *APOE*-4 heterozygotes had significant 2-year declines in regional brain activity, the largest of which was in temporal cortex, and that these reductions were significantly greater than those in *APOE*-4 noncarriers. Their findings suggest that as few as 22 cognitively normal, middle-aged *APOE*-4 heterozygotes would be needed in each treatment arm (i.e., active drug and placebo) to test a prevention therapy over a 2-year period (103).

Clinical Trials of Presymptomatic Patients Using Neuroimaging Surrogate Markers

The longitudinal findings of significant parietal and temporal metabolic decline in asymptomatic persons at risk of AD because of age or genetic risk or both have now been confirmed at two centers in separate subject cohorts. Together, these studies indicate that combining PET imaging of glucose metabolism and genetic risk may be useful outcome markers in AD prevention trials. Functional brain imaging techniques could be used to track preclinical cognitive decline and to test candidate prevention therapies without having to perform prolonged multisite studies using incipient AD as the primary outcome measure. The consistency and extent of the metabolic decline in these well-screened populations indicate that the PET measures provide adequate power to observe such decline in relatively small subject groups. A similar but less striking metabolic decline pattern was noted in subjects without *APOE*-4 such that larger groups per treatment arm would be needed.

These observations provide an opportunity for presymptomatic treatment trials not previously available. Until now, such trials involved studies of preclinical subjects with more severe memory impairments consistent with MCI, wherein approximately 50% of subjects actually develop dementia over a 3- to 4-year period. The MCI trials have required hundreds of subjects for adequate power. These trials use a categorical variable, incipient dementia, as the primary outcome measure. The introduction of FDG PET imaging combined with *APOE*-4 genetic risk increases efficiency and reduces costs by addressing the research questions with fewer subjects. Our group is currently performing two such placebo-controlled trials, one using the cyclooxygenase-2 inhibitor celecoxib and the other using the cholinesterase inhibitor donepezil.

Cost Benefit and Cost Effectiveness

Using neuroimaging as a surrogate marker early in the disease course, even in preclinical stages, has potential cost benefits beyond the greater efficiency in preclinical trials. Because FDG PET increases diagnostic sensitivity and specificity of AD (104), the technique could improve diagnostic homogeneity in clinical trials of mild to moderate AD. Rather than treating the conventional clinical syndrome of AD, the refined phenotype would include a specific neuroimaging pattern (e.g., parietal and temporal hypometabolism). If PET can improve diagnostic accuracy, particularly in the preclinical and early disease stages, then patients would be treated earlier, with resulting improvements in their daily functioning and quality of life. When uncertain about diagnosis, clinicians generally perform costly repetitive examinations. The greater accuracy of early AD detection that neuroimaging may offer would facilitate early intervention. Offsetting the pharmacy costs would be the cost savings from avoidance of repetitive and unnecessary examinations. Following evidence from placebo-controlled studies, the assessment of economic impact would be another level of analysis driving decision makers to fund new neuroimaging technologies. Definitive diagnosis and treatment

during presymptomatic stages of AD would likely decrease both direct and indirect costs. The improved diagnostic accuracy could improve efficacy in clinical trials and could thus facilitate early optimal treatment, delay further cognitive decline, and meet patient and family expectations of the highest-quality care.

ACKNOWLEDGMENTS

This work is supported in part by the following: the Alzheimer's Association, the Charles A. Dana Foundation, the Montgomery Street Foundation, San Francisco; the Fran and Ray Stark Foundation Fund for Alzheimer's Disease Research, Los Angeles; and National Institutes of Health grants MH52453, AG10123, and AG13308. The views expressed are mine and do not necessarily represent those of the Department of Veterans Affairs.

REFERENCES

1. Mant A, Eyland EA, Pond DC, et al. Recognition of dementia in general practice: comparison of general practitioners' opinions with assessments using the Mini-Mental State Examination and Blessed dementia rating scale. *Fam Pract* 1988;5:184–188.
2. McCartney JR, Palmateer LM. Assessment of cognitive deficit in geriatric patients: a study of physician behavior. *J Am Geriatr Soc* 1985;33:467–471.
3. Ross GW, Abbott RD, Petrovitch H, et al. Frequency and characteristics of silent dementia among elderly Japanese-American men: the Honolulu-Asia Aging Study. *JAMA* 1997;277: 800–805.
4. Ryan DH. Misdiagnosis in dementia: comparisons of diagnostic error rate and range of hospital investigation according to medical specialty. *Int J Geriatr Psychiatry* 1994;9:141–147.
5. Small GW, Komo S, La Rue A, et al. Early detection of Alzheimer's disease by combining apolipoprotein E and neuroimaging. *Ann NY Acad Sci* 1996;802:70–78.
6. Gibby WA, Zimmerman RA. X-ray computed tomography. In: Mazziotta JC, Gilman S, eds. *Clinical brain imaging: principles and applications.* Philadelphia: FA Davis, 1992:2–38.
7. Creasey H, Schwartz M, Frederickson H, et al. Quantitative computed tomography in dementia of the Alzheimer type. *Neurology* 1986;36:1563–1568.
8. de Leon MJ, George AE, Reisberg B, et al. Alzheimer's disease: longitudinal CT studies of ventricular change. *AJR Am J Roentgenol* 1989;152:1257–1262.
9. Shellock FG, Morisoli S, Kanal E. MR procedures and biomedical implants, materials, and devices: 1993 update. *Radiology* 1993;189:587–599.
10. Horn R, Ostertun B, Fric M, et al. Atrophy of hippocampus in patients with Alzheimer's disease and other diseases with memory impairment. *Dementia* 1996;7:182–186.
11. Leuchter AF, Spar JE, Walter DO, et al. Electroencephalographic spectra and coherence in the diagnosis of Alzheimer's-type and multi-infarct dementia. *Arch Gen Psychiatry* 1987;44: 993–998.
12. Dunkin JJ, Leuchter AF, Newton TF, et al. Reduced EEG coherence in dementia: state or trait marker? *Biol Psychiatry* 1994;35:870–879.
13. Dunkin JJ, Osato S, Leuchter AF. Relationships between EEG coherence and neuropsychological tests in dementia. *Clin Electroencephalogr* 1995;26:47–58.
14. Schuckit MA. An introduction and overview of clinical applications of NeuroSPECT in psychiatry. *J Clin Psychiatry* 1992; 53[Suppl]:3–6.
15. Mazziotta JC, Phelps ME. Positron emission tomography studies of the brain. In: Phelps M, Mazziotta J, Schelbert H, eds. *Positron emission tomography and autoradiography: principles and applications for the brain and heart.* New York: Raven, 1986: 493–579.
16. Mazziotta JC, Frackowiak RSJ, Phelps ME. The use of positron emission tomography in the clinical assessment of dementia. *Semin Nucl Med* 1992;22:233–246.
17. Silverman DHS, Small GW, Phelps ME. Clinical value of neuroimaging in the diagnosis of dementia: sensitivity and specificity of regional cerebral metabolic and other parameters for early identification of Alzheimer's disease. *Clin Positron Imaging* 1999;2:119–130.
18. Rinne JO, Sahlberg N, Ruottinen H, et al. Striatal uptake of the dopamine reuptake ligand [^{11}C]b-CFT is reduced in Alzheimer's disease assessed by positron emission tomography. *Neurology* 1998;50:152–156.
19. Meltzer CC, Smithy G, DeKosky ST, et al. Serotonin in aging, late-life depression, and Alzheimer's disease: the emerging role of functional imaging. *Neuropsychopharmacology* 1998;18: 407–430.
20. Nordberg A, Lundqvist H, Hartvig P, et al. Imaging of nicotinic and muscarinic receptors in Alzhiemer's disease: effect of tacrine treatment. *Dementia Geriatr Cogn Disord* 1997;8:78–84.
21. Weiner MW. NMR spectroscopy for clinical medicine, animal models, and clinical examples. *Ann NY Acad Sci* 1987;508: 287–289.
22. Schuff N, Amend D, Ezekiel F, et al. Changes of hippocampal *N*-acetyl aspartate and volume in Alzheimer's disease: a proton MR spectroscopic imaging and MRI study. *Neurology* 1997;49: 1513–1521.
23. Huang W, Alexander GE, Daly EM, et al. High brain myo-inositol levels in the predementia phase of Alzheimer's disease in adults with Down's syndrome: a 1H MRS study. *Am J Psychiatry* 1999;156:1879–1886.
24. Belliveau JW, Kennedy DN, McKinstry RC, et al. Functional mapping of the human visual cortex by magnetic resonance imaging. *Science* 1992;254:716–719.
25. Cohen MS, Bookheimer SY. Localization of brain function using magnetic resonance imaging. *Trends Neurosci* 1994;17: 268–277.
26. Demb JB, Desmond J, Wagner AD, et al. Semantic encoding and retrieval in the left inferior prefrontal cortex: a functional MRI study of task difficulty and process specificity. *J Neurosci* 1995;15:5870–5878.
27. Gabrieli JDE, Brewer JB, Desmond JE, et al. Separate neural bases of two fundamental memory processes in the human medial temporal lobe. *Science* 1997;276:264–266.
28. Stern CE, Corkin S, González RG, et al. The hippocampal formation participates in novel picture encoding: evidence from functional magnetic resonance imaging. *Proc Natl Acad Sci USA* 1996;93:8660–8665.
29. Schacter DL, Buckner RL, Koutstaal W, et al. Late onset of anterior prefrontal activity during true and false recognition: an event-related fMRI study. *Neuroimage* 1997;6:259–269.
30. Wagner AD, Schacter DL, Rotte M, et al. Building memories: remembering and forgetting of verbal experiences as predicted by brain activity. *Science* 1998;281:1188–1191.
31. Fox PT, Raichle ME. Focal physiological uncoupling of cerebral blood flow and oxidative metabolism during somatosensory

stimulation in human subjects. *Proc Natl Acad Sci USA* 1986; 83:1140–1144.
32. Ogawa S, Tank DW, Menon R, et al. Intrinsic signal changes accompanying sensory stimulation: functional brain mapping with magnetic resonance imaging. *Proc Natl Acad Sci USA* 1992; 89:5951–5955.
33. Backman L, Andersson JLR, Nyberg L, et al. Brain regions associated with episodic retrieval in normal aging and Alzheimer's disease. *Neurology* 1999;52:1861–1870.
34. Jones EK, Simmons A, Williams SCR, et al. Non-invasive assessment of axonal fiber connectivity in the human brain via diffusion tensor MRI. *Magn Reson Med* 1999;42:37–41.
35. Buchsbaum MS, Tang CY, Peled S, et al. MRI white matter diffusion anisotropy and PET metabolic rate in schizophrenia. *Neuroreport* 1998;9:425–430.
36. Virta A, Barnett A, Pierpaoli C. Visualizing and characterizing white fiber structure and architecture in the human pyramidal tract using diffusion tensor MRI. *Magn Reson Imaging* 1999; 17:1121–1133.
37. Hanyu H, Sakurai H, Iwamoto T, et al. Diffusion-weighted MR imaging of the hippocampus and temporal white matter in Alzheimer's disease. *J Neurol Sci* 1998;156:195–200.
38. Hanyu H, Shindo H, Kakizaki D, et al. Increased water diffusion in cerebral white matter in Alzheimer's disease. *Gerontology* 1997;43:343–351.
39. Small GW, Stern CE, Mandelkern MA, et al. Reliability of drawing regions of interest for positron emission tomographic data. *Psychiatry Res* 1992;45:177–185.
40. Pelizzari CA, Chen GTY, Spelbring DR, et al. Accurate three-dimensional registration of CT, PET and/or MR images of the brain. *J Comput Assist Tomogr* 1989;13:20–26.
41. Woods RP, Mazziotta JC, Cherry SR. MRI-PET registration with automated algorithm. *J Comput Assist Tomogr* 1993;17: 536–546.
42. Friston KJ, Ashburner J, Frith CD, et al. Spatial registration and normalisation of images. *Hum Brain Mapping* 1995;2: 165–189.
43. Friston KJ, Holmes A, Poline JB, et al. Detecting activations in PET and fMRI: levels of inference and power. *Neuroimage* 1996;4:223–235.
44. Minoshima S, Frey KA, Koeppe RA, et al. A diagnostic approach in Alzheimer's disease using three-dimensional stereotactic surface projections of fluorine-18-FDG PET. *J Nucl Med* 1995; 36:1238–1248.
45. Reiman EM, Caselli RJ, Yun LS, et al. Preclinical evidence of Alzheimer's disease in persons homozygous for the epsilon 4 allele for apolipoprotein E [see Comments]. *N Engl J Med* 1996; 334:752–758.
46. Rusinek H, de Leon MJ, George AE, et al. Alzheimer disease: measuring loss of cerebral gray matter with MR imaging. *Neuroradiology* 1991;178:109–114.
47. Müller-Gärtner HW, Links JM, Prince JL, et al. Measurement of radiotracer concentration in brain gray matter using positron emission tomography: MRI-based correction for partial volume effects. *J Cereb Blood Flow Metab* 1992;12:571–583.
48. Ibáñez V, Pietrini P, Alexander GE, et al. Regional glucose metabolic abnormalities are not the result of atrophy in Alzheimer's disease. *Neurology* 1998;50:1585–1593.
49. McKhann G, Drachman D, Folstein M, et al. Clinical diagnosis of Alzheimer's disease: report of the NINCDS-ADRDA Work Group under the auspices of Department of Health and Human Services Task Force on Alzheimer's Disease. *Neurology* 1984; 34:939–944.
50. Crook T, Bartus RT, Ferris SH, et al. Age-associated memory impairment: proposed diagnostic criteria and measures of clinical change. Report of a National Institute of Mental Health Work Group. *Dev Neuropsychol* 1986;2:261–276.
51. Larrabee GJ, Crook TH. Estimated prevalence of age-associated memory impairment derived from standardized tests of memory function. *Int Psychogeriatr* 1994;6:95–104.
52. Petersen RC, Smith GE, Waring SC, et al. Mild cognitive impairment: clinical characterization and outcome. *Arch Neurol* 1999;56:303–308.
53. Andersen K, Nielsen H, Lolk A, et al. Incidence of very mild to severe dementia and Alzheimer's disease in Denmark: the Odense Study. *Neurology* 1999;52:85–90.
54. Price JL, Morris JC. Tangles and plaques in nondemented aging and "preclinical" Alzheimer's disease. *Ann Neurol* 1999;45: 358–368.
55. Braak H, Braak E. Neuropathological stageing of Alzheimer-related changes. *Acta Neuropathol (Berl)* 1991;82:239–259.
56. Arai T, Ikeda K, Akiyama H, et al. A high incidence of apolipoprotein E ϵ4 allele in middle-aged non-demented subjects with cerebral amyloid beta protein deposits. *Acta Neuropathol (Berl)* 1999;97:82–84.
57. Snowdon DA, Kemper SJ, Mortimer JA, et al. Linguistic ability in early life and cognitive function and Alzheimer's disease in late life: findings from the nun study. *JAMA* 1996;275: 528–532.
58. Beach TG, Honer WG, Hughes LH. Cholinergic fibre loss associated with diffuse plaques in the non-demented elderly: the preclinical stage of Alzheimer's disease? *Acta Neuropathol (Berl)* 1997;93:146–153.
59. Shen J, Barnes CA. Age-related decrease in cholinergic synaptic transmission in three hippocampal subfields. *Neurobiol Aging* 1996;17:439–451.
60. Small GW, Ercoli LM, Huang S-C, et al. PET and genetic risk for Alzheimer disease. *J Nucl Med* 1999;40[Suppl]:70.
61. Small GW, Mazziotta JC, Collins MT, et al. Apolipoprotein E type 4 allele and cerebral glucose metabolism in relatives at risk for familial Alzheimer disease. *JAMA* 1995;273:942–947.
62. de Leon MJ, George AE, Golomb J, et al. Frequency of hippocampal formation atrophy in normal aging and Alzheimer's disease. *Neurobiol Aging* 1997;18:1–11.
63. Boone KB, Miller BL, Lesser IM, et al. Neuropsychological correlates of white-matter lesions in healthy elderly subjects. a threshold effect. *Arch Neurol* 1992;49:549–554.
64. Lopez OL, Becker JT, Rezek D, et al. Neuropsychiatric correlates of cerebral white-matter radiolucencies in probable Alzheimer's disease. *Arch Neurol* 1992;49:828–834.
65. Kesslak JP, Nalcioglu O, Cotman CW. Quantification of magnetic resonance scans for hippocampal and parahippocampal atrophy in Alzheimer's disease. *Neurology* 1991;41:51–54.
66. Pearlson GD, Harris GJ, Powers RE, et al. Quantitative changes in mesial temporal volume, regional cerebral blood flow, and cognition in Alzheimer's disease. *Arch Gen Psychiatry* 1992;49: 402–408.
67. Laakso MP, Soininen H, Partanen K, et al. MRI of the hippocampus in Alzheimer's disease: sensitivity, specificity, and analysis of the incorrectly classified subjects. *Neurobiol Aging* 1998; 19:23–31.
68. Pasquier F, Lavenu I, Lebert F, et al. The use of SPECT in a multidisciplinary memory clinic. *Dementia Geriatr Cogn Disord* 1997;8:85–91.
69. Pucci E, Belardinelli N, Regnicolo L, et al. Hippocampus and parahippocampal gyrus linear measurements based on magnetic resonance in Alzheimer's disease. *Eur Neurol* 1998;39:16–25.
70. Jack CR, Petersen RC, Xu YC, et al. Prediction of AD with MRI-based hippocampal volume in mild cognitive impairment. *Neurology* 1999;52:1397–1403.
71. Wahlund L-O, Julin P, Lindqvist J, Scheltens P. Visual assess-

ment of medial temporal atrophy in demented and healthy control subjects: correlation with volumetry. *Psychiatry Res Neuroimaging* 1999;90:193–199.
72. Killiany RJ, Moss MB, Albert MS, et al. Temporal lobe regions on magnetic resonance imaging identify patients with early Alzheimer's disease. *Arch Neurol* 1993;50:949–954.
73. Laakso MP, Partanen K, Riekkinen P, et al. Hippocampal volumes in Alzheimer's disease, Parkinson's disease, with and without dementia, and in vascular dementia: an MRI study. *Neurology* 1996;46:678–681.
74. Reiman EM, Uecker A, Caselli RJ, et al. Hippocampal volumes in cognitively normal persons at genetic risk for Alzheimer's disease. *Ann Neurol* 1998;44:288–291.
75. Erkinjuntti T, Gao F, Lee DH, et al. Lack of difference in brain hyperintensities between patients with early Alzheimer's disease and control subjects. *Arch Neurol* 1994;51:260–268.
76. Mauri M, Sibilla L, Bono G, et al. The role of morpho-volumetric and memory correlations in the diagnosis of early Alzheimer dementia. *J Neurol* 1998;245:525–530.
77. Bobinski M, de Leon MJ, Convit A, et al. MRI of entorhinal cortex in mild Alzheimer's disease. *Lancet* 1999;353:38–40.
78. Geroldi C, Pihlajamaki M, Laakso MP, et al. APOE-ϵ4 is associated with less frontal and more medial temporal lobe atrophy in AD. *Neurology* 1999;53:1825–1832.
79. Soininen H, Partanen K, Pitkanen A, et al. Decreased hippocampal volume asymmetry on MRIs in nondemented elderly subjects carrying the apolipoprotein E ϵ4 allele. *Neurology* 1995; 45:1467–1472.
80. Mattman A, Feldman H, Forster B, et al. Regional HmPAO SPECT and CT measurements in the diagnosis of Alzheimer's disease. *Can J Neurol Sci* 1997;24:22–28.
81. Jack CR, Petersen RC, Xu YC, et al. Hippocampal atrophy and apolipoprotein E genotype are independently associated with Alzheimer's disease. *Ann of Neurol* 1998;43:303–310.
82. Motter R, Vigo-Pelfrey C, Kholodenko D, et al. Reduction of beta-amyloid peptide 42 in the cerebrospinal fluid of patients with Alzheimer's disease. *Ann Neurol* 1995;38:643–648.
83. Ashburn TT, Han H, McGuinness BF, et al. Amyloid probes based on Congo red distinguish between fibrils comprising different peptides. *Chem Biol* 1996;3:351–358.
84. Klunk WE, Debnath ML, Pettegrew JW. Chrysamine-G binding to Alzheimer and control brain: autopsy study of a new amyloid probe. *Neurobiol Aging* 1995;16:541]]-548.
85. Lovat LB, O'Brien AA, Armstrong SF, et al. Scintigraphy with ^{123}I-serum amyloid P component in Alzheimer disease. *Alzheimer Dis Assoc Disord* 1998;12:208]]-210.
86. Majocha RE, Reno JM, Friedland RP, et al. Development of a monoclonal antibody specific for beta/A4 amyloid in Alzheimer's disease brain for application to *in vivo* imaging of amyloid angiopathy. *J Nucl Med* 1992;33:2184–2189.
87. Barrio JR, Huang S-C, Cole GM, et al. PET imaging of tangles and plaques in Alzheimer disease. *J Nucl Med* 1999;40[Suppl]: 70P–71P.
88. Jacobson A, Petric A, Hogenkamp D, et al. 1,1-Dicyano-2-(6-dimethylamino)naphthalen-2-yl)propene (DDNP): a solvent polarity and viscosity sensitive fluorophore for fluorescence microscopy. *J Am Chem Soc* 1996;118:5572–5579.
89. Wechsler D. *Wechsler memory scale,* rev. manual. San Antonio, TX: Psychological Corp., Harcourt Brace Jovanovich, 1987.
90. Parnetti L, Lowenthal DT, Presciutti O, et al. 1H-MRS, MRI-based hippocampal volumetry, and ^{99m}Tc-HMPAO-SPECT in normal aging, age-associated memory impairment, and probable Alzheimer's disease. *J Am Geriatr Soc* 1996;44:133–138.
91. Kuhl DE, Small GW, Riege WH, et al. Cerebral metabolic patterns before diagnosis of probable Alzheimer's disease. *J Cereb Blood Flow Metab* 1987;7[Suppl 1]:S406.
92. Small GW, La Rue A, Komo S, et al. Predictors of cognitive change in middle-aged and older adults with memory loss. *Am J Psychiatry* 1995;152:1757–1764.
93. Small GW, Ercoli LM, Silverman DHS, et al. Cerebral metabolic and cognitive decline in persons at genetic risk for Alzheimer's disease. *Proc Natl Acad Sci USA* 2000;97:6037–6042.
94. Pietrini P, Dani A, Furey ML, et al. Low glucose metabolism during brain stimulation in older Down's syndrome subjects at risk for Alzheimer's disease prior to dementia. *Am J Psychiatry* 1997;154:1063–1069.
95. Rossor MN, Kennedy AM, Frackowiak RS. Clinical and neuroimaging features of familial Alzheimer's disease. *Ann NY Acad Sci* 1996;777:49–56.
96. Johnson KA, Jones K, Holman BL, et al. Preclinical prediction of Alzheimer's disease using SPECT. *Neurology* 1998;50: 1563–1571.
97. Hughes CP, Berg L, Danziger WL, et al. A new clinical scale for the staging of dementia. *Br J Psychiatry* 1982;140:566–572.
98. Mielke R, Heiss W-D. Positron emission tomography for diagnosis of Alzheimer's disease and vascular dementia. *J Neural Transm* 1998;53[Suppl]:237–250.
99. Messa C, Perani D, Lucignani G, et al. High-resolution technetium-99m–HMPAO SPECT in patients with probable Alzheimer's disease: comparison with fluorine-18–FDG PET. *J Nucl Med* 1994;35:210–216.
100. Miller BL, Mena S, Daly J, et al. Temporal-parietal hypoperfusion with single-photon emission computerized tomography in conditions other than Alzheimer's disease. *Dementia* 1990;1: 41–45.
101. Bookheimer SY, Strojwas MH, Cohen MS, et al. Brain activation in older people at genetic risk for Alzheimer's disease. *N Engl J Med* 2000;343:450–456.
102. Smith CD, Andersen AH, Kryscio RJ, et al. Altered brain activation in cognitively intact individuals at high risk for Alzhiemer's disease. *Neurology* 1999;53:1391–1396.
103. Reiman EM, Caselli RJ, Chen K, et al. Tracking the decline in cerebral glucose metabolism in persons and transgenic mice at genetic risk for Alzheimer's disease. *Alzheimer Imaging Consortium* 2000.
104. Hoffman JM, Welsh-Bohmer KA, Hanson M, et al. FDG-PET imaging in pathologically verified dementia. *J Nucl Med* 2000.

Neuropsychopharmacology: The Fifth Generation of Progress. Edited by Kenneth L. Davis, Dennis Charney, Joseph T. Coyle, and Charles Nemeroff. American College of Neuropsychopharmacology © 2002.